

Supporting materials

Table of content

1. Experimental Section
 - 1.1. Reagents
 - 1.2. Table S1. Oligonucleotides used in this study
 - 1.3 Instruments
 - 1.4. Selection pathogens
 - 1.5. Growth of the pathogens
 - 1.6. RNA extraction
 - 1.7. Nucleic acid-based amplification (NASBA)
 - 1.8. Analysis of NASBA products
 - 1.9. Reverse transcription amplification
 - 1.10. Visual detection of the amplicons.
 - 1.11. Signal visualization using TLC-plates
2. Nucleic acid-based amplification (NASBA), **Fig. S1**
3. Analysis of *H.influenzae* (*H.i.*) and Cytomegalovirus (CMV) sequence by biPxD probe and PxDM, **Fig. S2**
4. Analysis of *Listeria monocytogenes* (*L.m.*) NASBA amplicons using six designs of biPxD probe, **Fig S3**
5. Principles of biPxD sensor design, **Fig. S4**
6. Selectivity of peroxidase-like DNA machine (PxDM), **Fig. S5, S6**
7. Analysis of RT-PCR reaction mixtures and detection of *H.i* and CMV by PxDM sensors, **Fig. S7**
8. Principles of PxDM sensor design, **Figs. S8, S9, S10**
9. References

1. Experimental Section

1.1. Reagents. DNase/RNase-free water was purchased from Dia-M and used for all buffers and oligonucleotides' stock solutions. The enzymes were purchased from New England Biolabs (Ipswich, MA). The following chemicals were used Tris-HCl (Helicon, Russia), pH 8.5, KCl (Helicon, Russia), MgCl₂ (Helicon, Russia), NTPs ((ATP, UTP, CTP, GTP), BioSan, Russia), dNTPs (dATP, dTTP, dGTP, dCTP), Evrogen, Russia), Dimethyl sulfoxide (DMSO) (Helicon, Russia), Bovine serum albumin (BSA) (Sigma, Germany), T7 RNA polymerase (SibEnzyme, Russia), MMLV reverse transcriptase (Evrogen, Russia), RNase H (NEB, USA), RNase inhibitor (BioSan, Russia), TLC aluminum plates silica gel 60 F (Switzerland). Bacterial and viral strains were obtained from collection of St. Petersburg Pasteur Institute, Russia, and All procedures were conducted following the standards of medical care adopted in Russia.¹ Cells were set in culture and RNA was extracted via a modified phenol-chloroform method and ExtractRNA reagent, Evrogen, LLC.

1.2. All oligonucleotides (Table S1) were custom-made by DNA Synthesis or Evrogen (Moscow, Russia).

Table S1. Oligonucleotides used in this study

Name ^[a]	Sequences 5'→3' ^a	Comments
L.m._DNA	AGA ATT CGC TTA CCG CTA CTT GTA TTT TTA GCA ATA GCC GCA TTT CCT TTA ACT AAA ATA TAT ACT TTC GTT ACT TCA TCT GTA TAA A	Synthetic DNA analyte
L.m._DNA_mis match	AGA ATT CGC TTA CCG CTA CTT GTA TTT TTA GCA ATA GCC GCA TTT CCT TTA ACT AAA ATA TAT ACT TTC GTT ACT TCA TCT GTA TAA A	PxDm
L.m._DNA_antisense	TTTATACAGATGAAGTAACGAAAGTATATATTTTAGTTAAAGGAAATGCG GCTATTGCTAAAAATACAAGTAGCGGTAAGCGAATTCT TGATCT	PxDm
L.m._P1	aattctaatacgactcactatagggAGA ATT CGC TTA CCG CT	NASBA primer
L.m._P2	AAATATGTCTACTTCATTG	NASBA primer
L.m._F-1	GGG TT GGG ttttt A TAC AAG TAG CG acc	biPxD
L.m._M-1	AAA TGC GGC TAT TGC TAA AA ttttt GGG TA GGG	biPxD
L.m._F-2	GGG TA GGG ttttt A AAA TAC AAG TAG CGG TAA G	biPxD
L.m._M-2	aacc GC TAT TGC TA ttttt GGG TT GGG	biPxD
L.m._F-3	GGG TT GGG ttttt GTA TAT ATT T acc	biPxD
L.m._M-3	ATA CAG ATG AAG TAA CGA AA ttttt GGG TA GGG	biPxD
L.m._F-4	GGG TA GGG ttttt GAA GTA ACG AAA GTA TAT AT	biPxD
L.m._M-4	aacc TTA TAC AGA T ttttt GGG TA GGG	biPxD
L.m._M-5	GGG TT GGG ttt ttt GC TAA AA A TAC AAG TAG CG GTAAGCGAATTCT	biPxD
L.m._M-5	cctGTTAAA GGAAA TGC GGC TAT T ttt ctt GGG TA GGG	biPxD
L.m._M-6	GGG TTG GG /iSp9/ GCT AAA AAT ACA AGT AGC GGT AAG CGA ATT Cc	biPxD
L.m._F-6	GTT AAA GGA AAT GCG GCT ATT ctaa GGGTAGGG	biPxD
L.m._M-7	GG AAA TGC GGC TAT TG/iSp9/ GGGTAGGG	PxDm
L.m._T1 PxDm	G CGG T AAG CG AAT TC ttt CAC ACG TGTC TGTC	PxDm
L.m._T2 PxDm	GGGTTGGG /iSp9/ CTAAAAATACAAGTA ccc GAACA GAACA CGTGTG	PxDm
H.i._DNA	GGT TAT TTA AGT G AG GTG T GA AAG CCC TGG GCT TAA CC T AGG AAT TGC ATT TCA GAC TGG GTA ACT AGA GTA CTT TAG GGA G GG GTA GAA TT	Synthetic DNA analyte
H.i._P1	AATTCTAATACGACTCACTATAGGG AAT TCT ACC CCT CCC TAA	NASBA primer
H.i._P2	CCAATAAATTCCTCCA	NASBA primer
H.i._F-1	GGG TA GGG ttttt ACC TAG GAA TTG CAT TTC AG	biPxD
H.i._M-1	GCC CTG GG CTT A ttttt GGG TT GGG	biPxD
H.i._F-2	GGG TT GGG /iSp9/ CAG GGC TTT C	biPxD
H.i._M-2	cca GCA ATT CCT AGG TTA AGC C/iSp9/ G GGT AGG G	biPxD
H.i._M PxDm	GTC TGA AAT GCA ATT CCT AG /iSp9/ GGGTAGGG	PxDm
H.i._T1 PxDm	GGG CTT TCA CAC CTC ttt C ACA CGT GTT CTG TTG	PxDm
H.i._T2 PxDm	GGG TTG GG /iSp9/G TTA AGC CC /iSp9/CAA CAG AAC ACG TGT G	PxDm
CMV_DNA	C GT GAT CTT TCT TTT AC T TTG T TC ATA CAA ATA ATT CGT CGT ACA CCC	Synthetic DNA

	CGA TTA TCC CCC CTA TTG ACT CCA TAT C GT TGA TAC TTT	analyte
CMV_DNA2	AAC ACG TGG CTA AGG TAC AAC CTA TTT AC T CAA CGT AAC AAC GGT AGA C AT GAA GAA AA C CAA GAT AAT ACT CAT TCT A	Synthetic DNA analyte
CMV_P2	AAAGTATCAACGATATG	NASBA primer
CMV_P1	aattctaatacgaactcactatagggCGTGATCTTTCTTTTAC	NASBA primer
CMV_F-1	cct GTC TAC CGT TGT TAC GTT GA tttttt GGG TA GGG	biPxD
CMV_M-1	GGG TT GGG tttttt GTA AAT AGG TT	biPxD
CMV_F-2	GGGTA GGG /iSp9/ AAC AAA GTA AAA GAA AG	biPxD
CMV_M-2	cct AAT TAT TTG TAT G /iSp9/ GGG TT GGG	biPxD
CMV_M_PxDm	ACG ACG AAT TAT TTG TAT GA /iSp9/ GGGTAGGG	PxDm
CMV_T1_PxDm	AGA AAG ATC AC ttt GAC GCT GCA GA	PxDm
CMV_T2_PxDm	GGGTTGGG /iSp9/ ACA AAG TAA A ccc TCTGCAGCGTC	PxDm
L.m. M-8	C GGC TAT TG/iSp9/ GGGTAGGG	PxDm
L.m. M-8'	C GGC CAT TG/iSp9/ GGGTAGGG	PxDm
CMV_M-3	T TTG TAT GA /iSp9/ GGGTAGGG	PxDm
CMV_M-3'	T TTG CAT GA /iSp9/ GGGTAGGG	PxDm
L.m. M-9	GGC TAT TG TTTTTT GGGTAGGG	PxDm
L.m. M-9'	GGC CAT TG TTTTTT GGGTAGGG	PxDm

[a] 'p' – 5'-end phosphate group; /iSp9/, triethylene glycol linkers. Underlined nucleotides of the probe sequences are complementary to the analytes. Sequences of synthetic analytes corresponded to the sequences of amplicons; small cases indicate the sequence of T7 RNA polymerase promoters. Red letters are highlighted as introduced mismatches to the analyte.

1.3. Instruments. The melting temperatures and the oligonucleotides' extinction coefficients were predicted using DinaMelt and IDT (OligoAnalyzer Tool) software. The optical density of the samples was recorded on an Implen NanoPhotometer 80 ($\lambda = 500$ nm). Signal to background ratio was obtained via ImageJ software. The data was processed using Microsoft Excel, Origin Pro, and a homemade program in Jupiter Notebook.

1.4. Selection of pathogens. *L.monocytogenes*, *H.influenzae*, and Cytomegalovirus are pathogens responsible for a number of human diseases, such as listeriosis, acute respiratory viral infections, inflammation of various internal organs, pneumonia, and bronchitis. For identification of bacterial agents, we chose specific genes that are constitutively expressed and selective for the particular organism. As for the viral agent, we have tested various genes related to the late lytic cycle primarily associated with a capsid's proteins and an envelope. To identify *L. monocytogenes*, we have chosen the specific target gene Lmo0753. It has been shown that Lmo0753 assumes a crucial role in the virulence of *L. monocytogenes*.² This gene is commonly used in different amplification methods such as PCR and NASBA. To detect the *H.influenzae* we chose a 16S rRNA specific region.^{3,4} The UL_37 specific and well-presented gene was selected to detect Cytomegalovirus, since it confers resistance to apoptosis and may play a key role in an additional mechanism of antiviral resistance.⁵ The UL_55 gene is responsible for the envelope glycoprotein that forms spikes at the surface of the virion envelope. It was demonstrated that UL_55 is expressed early in the infectious cycle⁶, so identifying Cytomegalovirus was also tested.

1.5. Growth of the pathogens. Thus, *L.monocytogenes*, *H.influenzae* were grown at 37° C on Columbia agar with 5% sheep blood in 8-10% CO₂ overnight. For Cytomegalovirus cultivation were used Vero (ECACC 84113001) cell line. The line was grown at 37 °C with 5% CO₂ in α -MEM media containing 10% FBS (Thermo Fisher Scientific Inc), penicillin, and streptomycin (Biolot). Infection material was added in overnight cell cultures when the thickness of the monolayer was 80%. Samples of infected cultures were taken for RNA extraction after 18 h of cultivation before releasing viral particles from cells.

- 1.6. **RNA extraction.** According to the manufacturer's instructions, the bacterial and cell suspensions were homogenized in 1 mL of the Extract RNA solution (Evrogen) followed by RNA isolation.
- 1.7. **Nucleic acid-based amplification (NASBA).** The specific primer (P1 for L.m., H.i., CMV, Table S1) was hybridized with RNA. Besides the complementary RNA target sequence, this primer also contained the T7 RNA-polymerase sequence. The standard reaction included: 40 mM Tris pH 8.5, 2.5 mM Potassium chloride, 12 mM magnesium chloride, 2 mM of each nucleotide triphosphate (ATP, UTP, CTP, GTP), 1 mM of each deoxynucleotide triphosphate (dATP, dTTP, dGTP, dCTP), 5 μ M of each oligonucleotide primers, 15% dimethyl sulfoxide (DMSO), 30 units of T7, 30 units of MMLV reverse transcriptase, 0.3 units of RNase H, 3 μ g bovine serum albumin (BSA). At 41°C, AMV-RT lengthens this primer, creating a DNA copy from the RNA matrix and forming an RNA/cDNA hybrid. RNAase H takes this hybrid as a substrate and hydrolyses RNA, leaving a single-strand DNA with which the second primer (P2 for L.m., H.i., CMV) is hybridized. The mechanism produces multiple copies of RNA from the target RNA⁷. Thus, 1 μ L of the template was added regularly. Incubation was performed at 41°C for 60-90 min. In our experiments, the dithiothreitol (DTT) was omitted due to its interference with H₂O₂ in later experiments. Analyze by agarose gel electrophoresis (2% in TBE), 60 V, 60 min. Analyzed RNA in an amount of about 100 copies (Fig. S1).
- 1.8. **Analysis of NASBA products.** The analysis's efficacy was determined by the NASBA serial dilution of known amounts of bacterial or viral cells. The outputs were deemed positive if the change from colorless to a brownish solution was performed for a certain RNA and the optical density improved over 3 times as opposed to the negative control. The number of bacterial cells per mL was calculated and made dilutions corresponding to 10⁵, 10⁴, 10³, 100, 10, 1, or 0 of the bacterial cells per NASBA reaction were made. Three replicates were performed for each reaction. It should be noted that in the case of viral cells, the technology implied the use of still unformed viral particles. Therefore, to determine the genomic equivalents from which the RNA analysis was performed, we estimated the number of cells in the monolayer before infection with the virus. In the case of viruses, we diluted the monolayer cells to a minimum of 10,000 copies, and all subsequent reductions in genomic equivalents were carried out in decimal dilutions. With a decrease in the passage of cells less than 10,000, it was impossible to maintain and infect the culture. When isolating RNA at the final stage, the resulting precipitate containing RNA was dissolved in 10 μ L of NASBA reaction mixture, which means that 1 μ L contained about 1/10 of the genomic equivalents of the initial number of cells.
- 1.9. **Reverse transcription amplification.** Two solutions were prepared before amplification: Solution 1: 1 μ L of RNA (0.5-2 μ g); 1 μ L (20 μ M) of P1 (L.m., H.i., CMV, see Table1, respectively); 1 μ L RNase inhibitors; nuclease free water to 9 μ L.; Solution 2: 4 μ L of 5X first strand buffer (Evrogen, Russia); 2 μ L of dNTP mix (10 mM each, Evrogen, Russia); 2 μ L of DTT (20 mM, Evrogen, Russia); 1 μ L of M-MLV revertase (100 U/ μ L, Evrogen, Russia); nuclease free water to 11 μ L. Solution 1 was incubated at 70°C for 2 min and cooled on ice. Afterward, Solution 1 was mixed with Solution 2. 1 μ L of RNase inhibitor (20 U/ μ L, ThermoFisher, USA) was added. The mixed solution was incubated at 37-42°C for 30-60 min followed by heating at 70 °C for 10 min to stop the reaction. This protocol was used to synthesize the first strand of RNA into cDNA. Subsequently, the cDNA product was used for PCR and accumulation of the product for analysis by biPxD and PxDm sensors. The following reagents were used for the PCR: 2 μ L cDNA; 0.75 μ L Taq DNA polymerase (Evrogen, Russia); 2 μ L 10 x Taq Buffer (Evrogen, Russia); 0.4 μ L dNTP mix (10 mM each, Evrogen, Russia); 0.5 μ L primers (20 μ M); water up to 20 μ L. The reaction was carried out under the following conditions: preliminary denaturation (92 °C - 2 min); 35 cycles of denaturation (92 °C - 15 s), annealing (40 °C - 15 s), and elongation (72 °C - 20 s); final elongation (72 °C - 3 min). Products of amplification were analyzed by electrophoresis in 2% agarose, 1x TBE buffer.
- 1.10. **Visual detection of the amplicons.** Hereinafter, we compared these two technologies' output work: the mPxD with the most promising biPxDs sensors we have developed for this task. The detection with biPxDs and PxDms was held in the reaction buffer (50 mM HEPES, pH 7.4, 50 mM MgCl₂, 20 mM

KCl, 120 mM NaCl, 0.03% Triton X-100, 1% DMSO) by adding a strands M and F 1 μ M each (L.m_F-6 and L.m_M-6 for *L.monocytogenes*, H.i_F-2 and H.i_M-2 for *H.influenzae* detection, and CMV_F-2 and CMV_M-2 for Cytomegalovirus detection), DAB 1 μ M, H₂O₂ 1%, 1 μ M and hemin 1 μ M. As negative control NASBA reaction mixture containing no RNA input was used, as a positive control, a sample with 1 μ M of synthetic analyte (L.m_DNA for *L.monocytogenes* detection, H.i_DNA for *H.influenzae* detection, and CMV_DNA for Cytomegalovirus detection) was applied. Samples were incubated at room temperature (23-25°C) for 10 min with the following visual assay. The detection with PxDMs was held in the reaction buffer as well by adding strands T2, T1, and M 1 μ M each (L.m_T1_PxDm, L.m_T2_PxDm, L.m_M-7 strand for *L.monocytogenes*, H.i_T1_PxDm, H.i_T2_PxDm H.i_M_PxDm for *H.influenzae* detection, and CMV_T1_PxDm, CMV_T2_PxDm strand, CMV_M_PxDm for Cytomegalovirus detection), DAB 1 μ M, H₂O₂ 1%, 1 μ M, and hemin 1 μ M. As a negative control, NASBA reaction mixture containing no RNA input was used, as a positive control, a sample with 1 μ M of synthetic analyte (L.m_DNA for *L.monocytogenes* detection, H.i_DNA for *H.influenzae* detection, and CMV_DNA for Cytomegalovirus detection) was applied. Samples were incubated at room temperature (23-25°C) for 10 min with the following visual assay. The optical density of the samples was recorded on an Implen NanoPhotometer 80 (λ = 500 nm).

1.11. Signal visualization using TLC-plates

Solution assays were performed in TLC aluminium plates. For specific NASBA product detection, 20 μ L of a mix of DNA-sensing probes M-, F-strands for biPxDM or Arm 1, Arm 2 and Arm 3 for PxDM (1 μ M each probe) as well as 1 μ L of NASBA mixture (the rest volume was padded with a buffer). The solution was pipetted on the TLC plate and incubated for 10 min. Then, 1 μ L of hemin solution (1 μ M) was added and incubated for 5 min. Finally, 1 μ L H₂O₂ solution (1 mM), and 1 μ L DAB solution (1 mM) were pipetted. The concentrations were previously optimized for this reaction, as well as the type of probe used for the assay. The color difference was measured additionally to optical density with the ImageJ software.

2. Nucleic acid-based amplification (NASBA), Fig. S1

The number of bacterial and viral cells per μ l was calculated and complete dilutions are corresponding to 10⁵, 10⁴, 10³, 100, 10, 1 or 0 of the cells per NASBA reaction were made. Three replicates were performed for each reaction. Amplicons were quantified by densitometric scanning of the agarose gels using Chemi Doc™ Touch Imaging system (Bio-Rad) (Fig. S1, A, B).

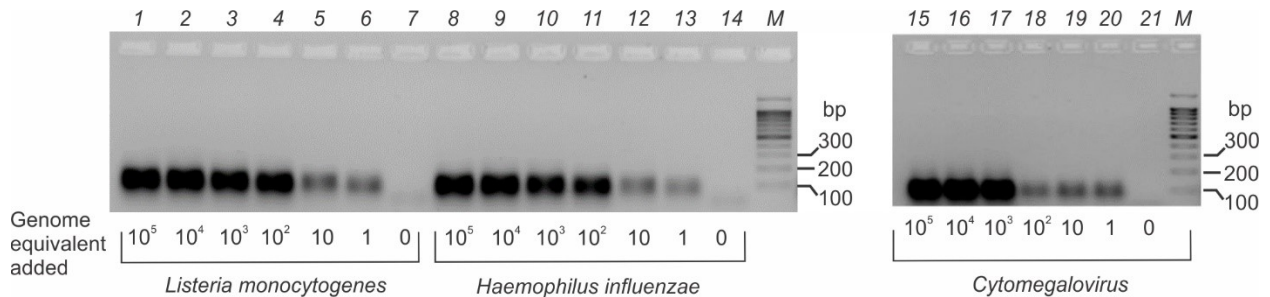


Fig. S1. Analysis of NASBA reaction mixtures by agarose 2%. **(A)** NASBA amplification of *L.monocytogenes* (lanes 1-6) (from 10⁵ to single genome equivalent (g.e.)), 7 - *L.monocytogenes* negative control: no sample added in isothermal PCR; 8 -13 *H.influenzae* (from 10⁵ to single g.e. respectively), 14 - *H.influenzae* negative control: no sample added in NASBA; M – ladder; **(B)** 15 - 20 Cytomegalovirus (from 10⁵ to single g.e. respectively), 21 - Cytomegalovirus negative control: no sample added in NASBA; M – ladder; agarose gel 2% in 1×TBE, 30 min, 80V NASBA amplicons.

3. Analysis of *H.influenzae* (H.i.) and *Cytomegalovirus* (CMV) sequence by biPxD probe and PxDM, Fig. S2

A possible explanation for the low S/B ratio of H.i. analyte using a biPxD probe can be a high cross-linking between both hybridization probes. With the PxDM probe, we eliminated the need for a design a long F-strand around a stable hairpin, thereby reducing the background and binding energy of the hybridization arms between each other. To detect CMV, we had to eliminate the possibility for binding with the primers in the NASBA reaction mixture. We moved the analyte-binding and G-4-forming arms of the sensor further away from the ends of the target area, which probably reduced the background. In turn, the signal intensity increased since the PxDM sensor binding most of the analyte length, increasing the selectivity of analyte detection in solution.

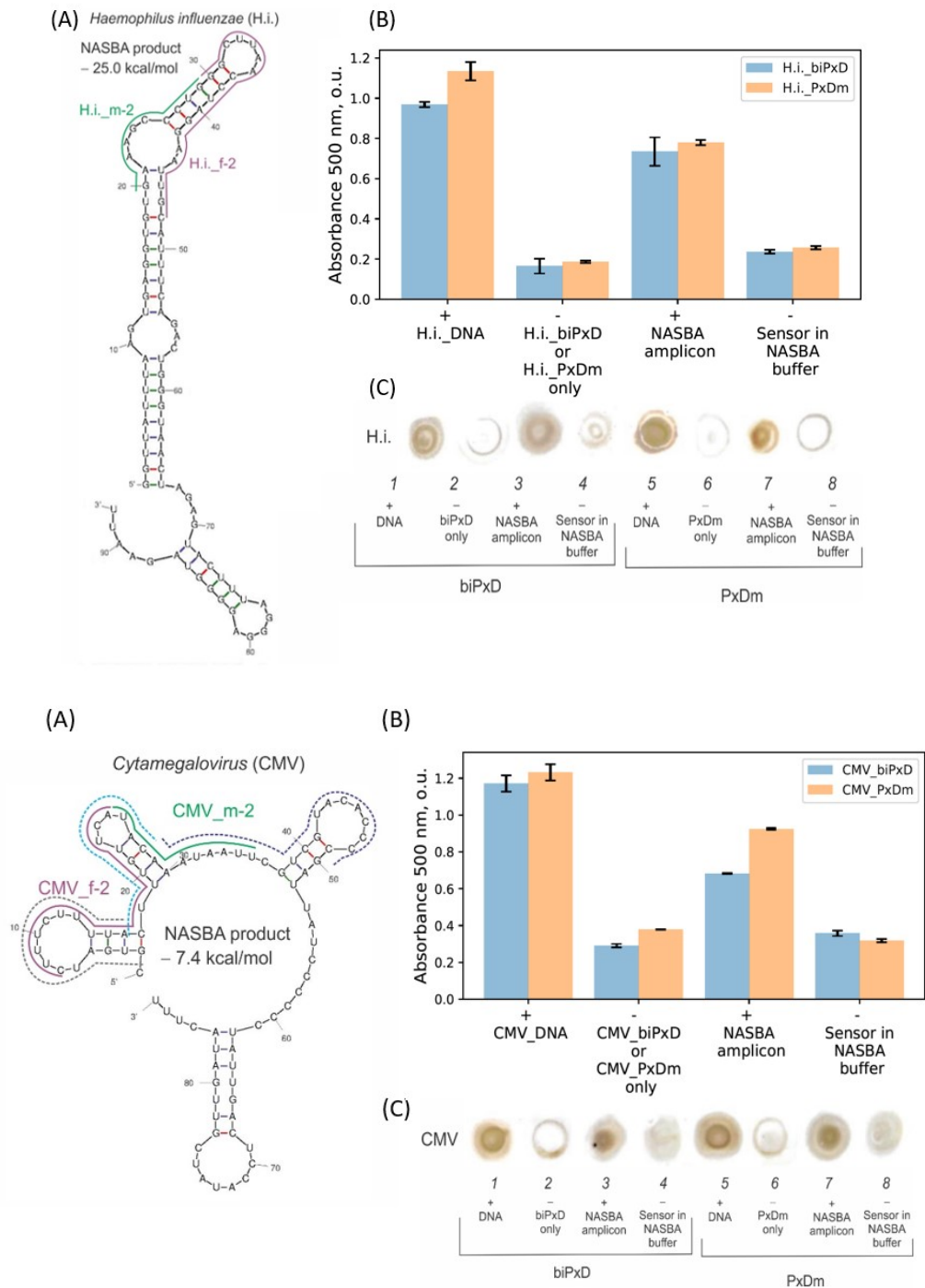


Fig. S2. Analysis of *H.influenzae* (H.i.) and Cytomegalovirus (CMV) sequence by biPxD probe and PxDM. A) Secondary structure of the NASBA amplicon predicted by UNAFold.⁸ Dashed, and dotted lines indicate nucleotides complementary to biPxD and PxDM, respectively. B) Sample absorbance at 500 nm. The data are average of 3 independent experiments. Colorimetric signal produced by biPxD probe and PxDM in the absence or presence of *H.influenzae* or Cytomegalovirus analytes. Bars 1 contained DNA analyte is a synthetic all-DNA, H.i._DNA or CMV_DNA (Table S1). The data of three independent experiments is presented. Minimal energy secondary structures of the DNA analytes. C) samples spotted on a TLC plate.

4. Analysis of *Listeria monocytogenes* (L.m.) NASBA amplicons using six designs of biPxD probe, Fig. S3

In designs 5 and 6, the position of the analyte-binding arms was identical; however, in the 5th design we added additional nucleotides to the ends of the individual arms to achieve folding into a stable secondary structure for each sensor part. Apparently, in this case, it turned out to be ineffective since each of the arms was significantly lengthened: probably the preferable reaction was not binding to the analyte, but the preservation of a stable secondary structure for each of the added arms. In addition, in the 6th design, a chemical linker was used, which most likely allowed the sensor flexibly to attach to the analyte and form the G-4 structure at the transition from the “stem” to the “loop”. At the same time, the colorimetric reaction in the NASBA solution did not work out in a favorable way due to the content of primers complementary to the f-strand of the analyte. As expected, shorter arms (design 1-2) did not show their detection ability even in the case of a synthetic analyte. Besides, designs 3-4 also did not give a statistically positive result, which may be since the “stem-loop” structure formed at the 3'-end of the analyte is not stable, and in the second variant, a possible secondary conformation obtained with UnaFold was not presented. This may indicate poor accessibility of the area for the sensor in the solution.

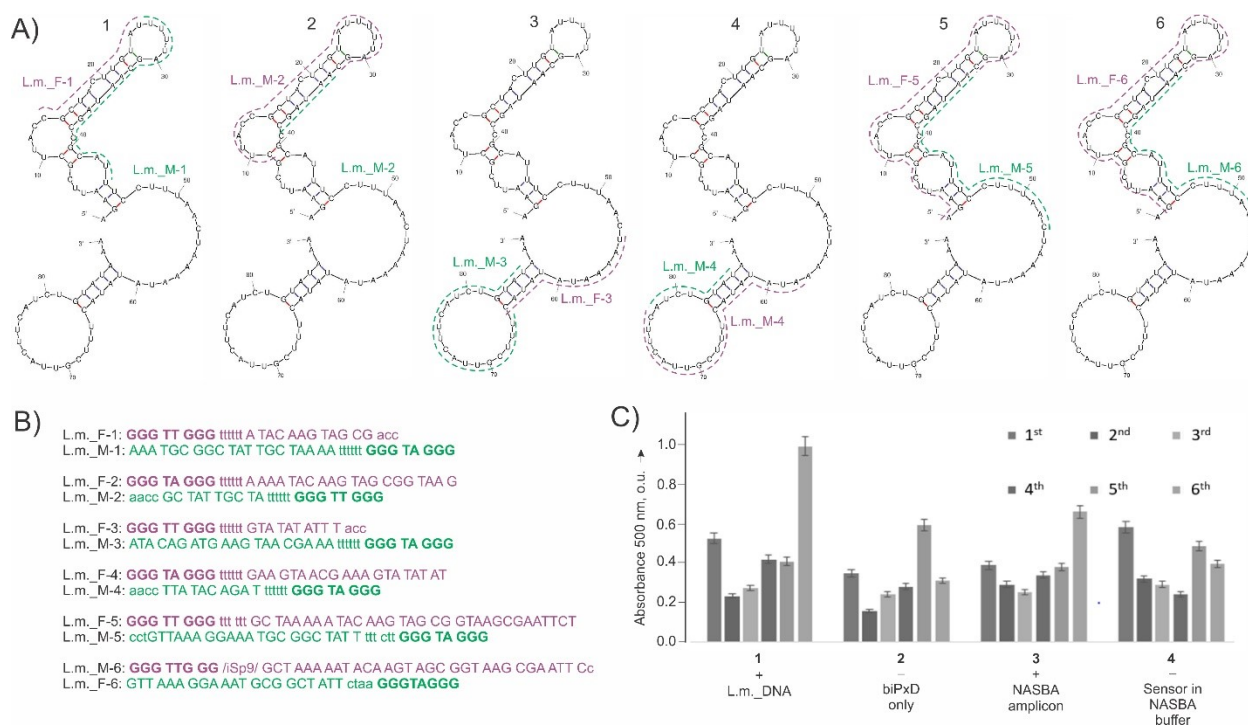


Fig. S3. Analysis of *Listeria monocytogenes* (L.m.) NASBA amplicon using six designs of BiPxD probe. A) Location of analyte-binding arms of strand M and F on the analyte secondary structure. B) Primary sequence of strands M and F. G-quadruplex forming sequences are in bold. C) Absorbance at 500 nm generated by the BiPxD probes in the absence or presence of either synthetic analyte (group 1 bars) or NASBA RNA amplicon (bar group 3). The data are average values of three independent measurements.

5. Principles of biPxD sensor design, Fig.S4

For comparative detection, we used a G-4 probe divided into 2 parts (biPxD) and connected through a spacer (triethylene glycol) to an oligonucleotide sequence that recognizes the target single-stranded DNA or RNA (analyte). In the absence of analyte 2 parts of G-4 exist mainly in dissociated form (at certain concentrations and incubation conditions). When 2 parts of G-4 are added to the analyte solution, they assemble into a complex structure and acquire peroxidase activity upon hybridization

with the analyte. Active peroxidase catalyzes a colorless substrate's oxidation (in this case, diaminobenzidine (DAB)) to a colored product.⁹

Figure 2 represents biPxD designs proposed earlier. It has also been designed to detect *L.monocytogenes*, *H.influenzae*, and Cytomegalovirus. For comparative analysis, the detection performance of biPxD and PxDM technology will be shown.

All structures were folded at 23°C. Different Gibbs energy¹⁰ is required for the folding: its absolute meaning is highlighted on the Fig. S4.

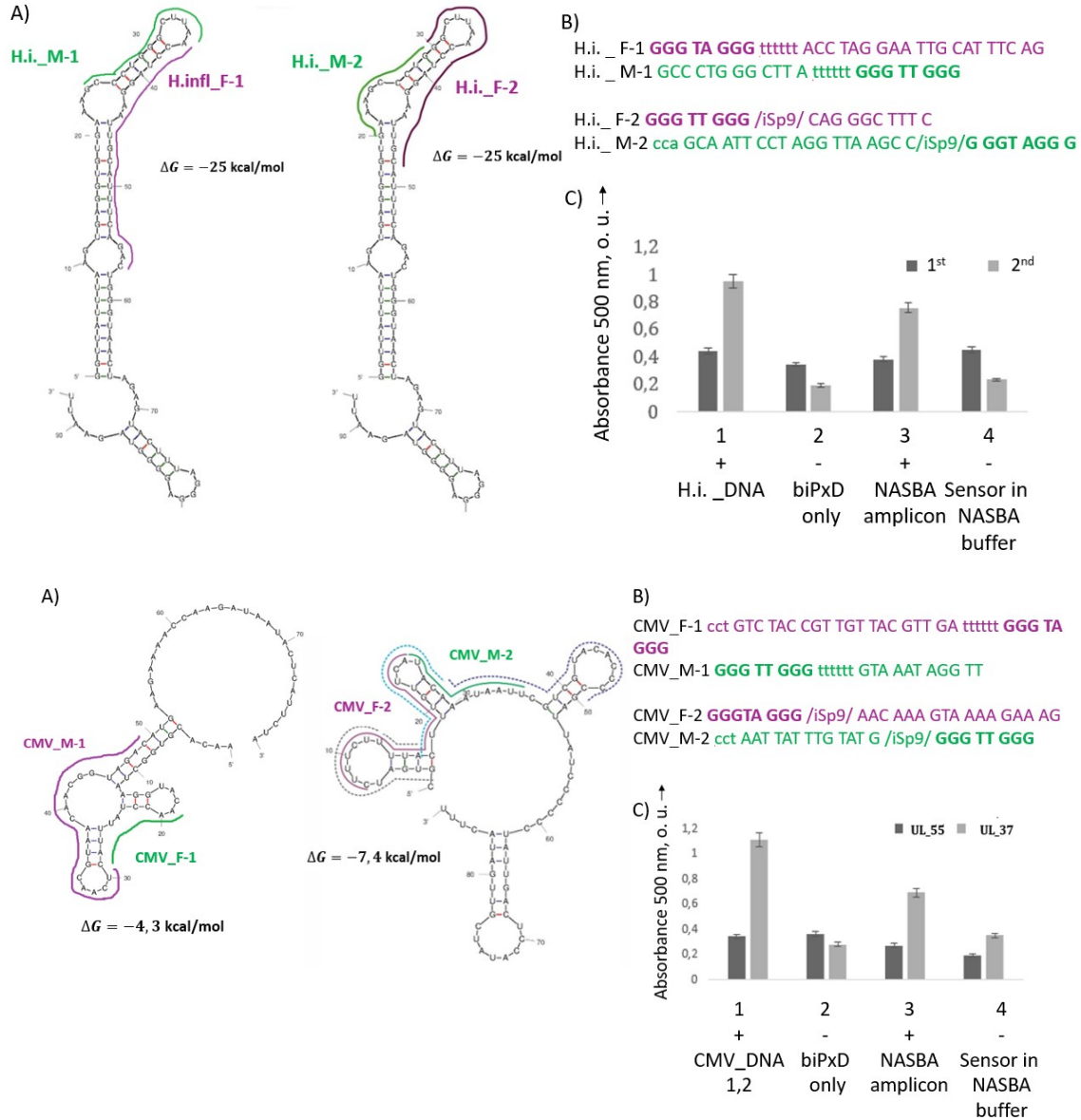


Fig. S4. Analysis of *H. influenzae*, and Cytomegalovirus (H.i._DNA, CMV_DNA1, 2) NASBA amplicons different designs of BiPxD probe. A) Location of analyte-binding arms of strand M and F on the analyte secondary structure. B) Primary sequence of strands M and F. G-quadruplex forming sequences are in bold. C) Absorbers at 500 nm generated by the BiPxD probes in the absence or presence of either synthetic analyte (group 1 bars) or NASBA RNA amplicon (bar group 3). The data are average values of three independent measurements.

First, the biPx_D probes' output was optimized using synthetic RNA oligonucleotides that matched the sequence with the target amplicons *H. influenzae*, and Cytomegalovirus (H.i._DNA, CMV_DNA in Table 1). The F-strand analyte binding arms were designed to be long enough to have high binding affinity while still unwinding the analyte RNA secondary structure (Fig. S4). On the other hand, Strands M had short analyte-binding arms, allowing hybridization only to entirely complementary sequences under the hybridization conditions. Go over the main points, such a design was shown to have both high binding affinity to folded nucleic acids and high analyte recognition selectivity.^{10,12} A hexaethylene glycol spacer attached the analyte binding arm and the G-4-forming fragment, enabling designing the G-4 structure in close proximity to the bulk probe-analyte complex. Both strands M and F were supplemented with non-complementary nucleotides to the analyte to decrease their associations in G-4 in the absence of analytes. Since for *L. monocytogenes* and Cytomegalovirus RNA hairpins are positioned near the analyte ends, the design of a biPx_D for a given analyte's confirmation is complicated. This is not a critical concern in detecting a synthetic analyte; however, there is a possibility of cross-hybridization with primers in the case of the detection of amplified RNA. Probes with strands without intramolecular folding gave a substantial background color change in the absence of analytes.

6. Selectivity of peroxidase-like DNA machine (Px_{Dm}), Fig. S5, S6

To demonstrate the selectivity of the approach, we introduced mismatched bases in analyte-binding arms M for L.m. and CMV, strands L.m._M-8' and CMV_M-3' in the table S1, respectively. Therefore, the previously created M-strands were initially reduced to 9-10 nucleotides before being replaced with L.m. M-8 and CMV M-3. Following that, SNPs (single nucleotide substitutions) were inserted into designed strands (L.m. M-8' and CMV M-3'). Such a mismatch employing M strands having miss matches to CMV and L.m. analytes, particularly with the introduction of replacement for C, causes the short arm's binding to the analyte to be markedly hindered, and the analyte + arms + G-quadruplex complex to be not assembled at all or becomes unstable. It leads to the occasional notable drop of the colorimetric signal to the background level.

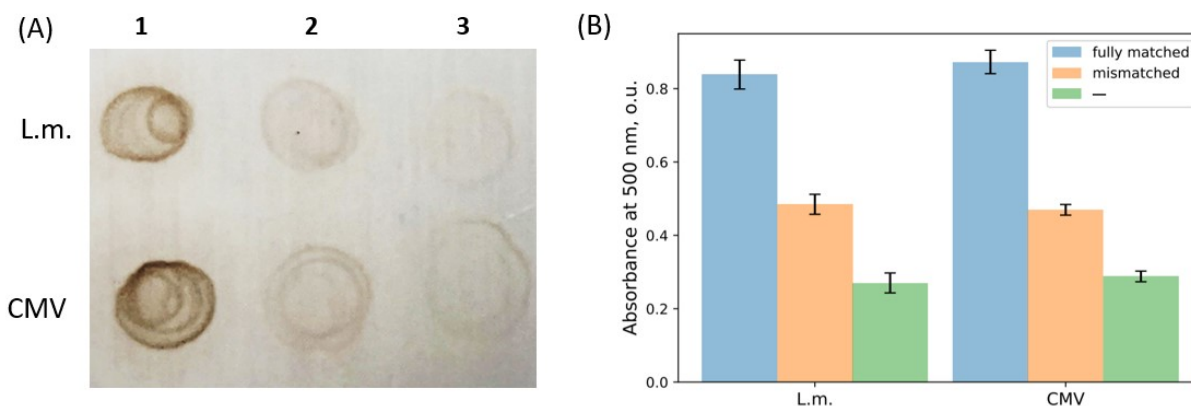


Fig. S5. Selectivity of peroxidase-like DNA machine (Px_{Dm}). A) Visual detection of *L.monocytogenes* and Cytomegalovirus NASBA amplicons by multicomponent (Px_{Dm}) sensor with 1) fully-matched M-strand 2) mismatched M-strand in comparison with negative control (NASBA mixture with reagents and sensor without bacterial RNA). Visualization of the color change in the reaction mixtures containing NASBA amplicons obtained from 100 cells of *L.monocytogenes* and Cytomegalovirus (Vero cell line). B) Absorbance measurements of negative NASBA control (sensor and reagents in NASBA mixture without bacterial RNA), fully-matched/mismatched strands with NASBA products of *L.monocytogenes*, Cytomegalovirus.

Discrimination of a single mutation is considered to be the most challenging practically significant task for hybridization sensors. The initially designed PxDM reliable differentiation of single base-substituted form fully complementary (Fig.S5). To further reduce the response to a mismatched analyte, we shortened the Arm 1 to 8 nucleotides, which led to even higher signal drop from the mismatched analyte to the level indistinguishable from the background (Fig. S6).

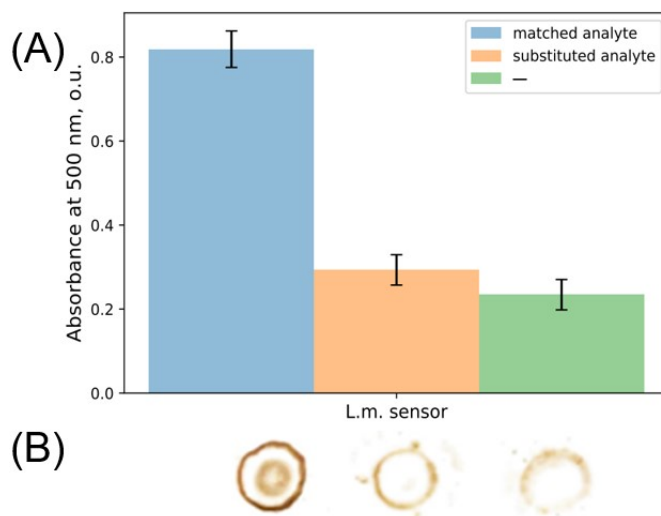


Fig. S6. A) Absorbance measurements of negative control (sensor and all the reagents in the buffer), fully-matched/mismatched (M-9, M-9') strands with fully-matched/mismatched L.m._DNA. B) Visual detection of fully-matched/mismatched L.m._DNA by multicomponent (PxDM) sensor with 1) fully-matched M-9 2) mismatched M-9' in comparison with negative control.

7. Analysis of RT-PCR reaction mixtures and detection of *H.influenzae*, 3- Cytomegalovirus by PxDm sensors, Fig. S7

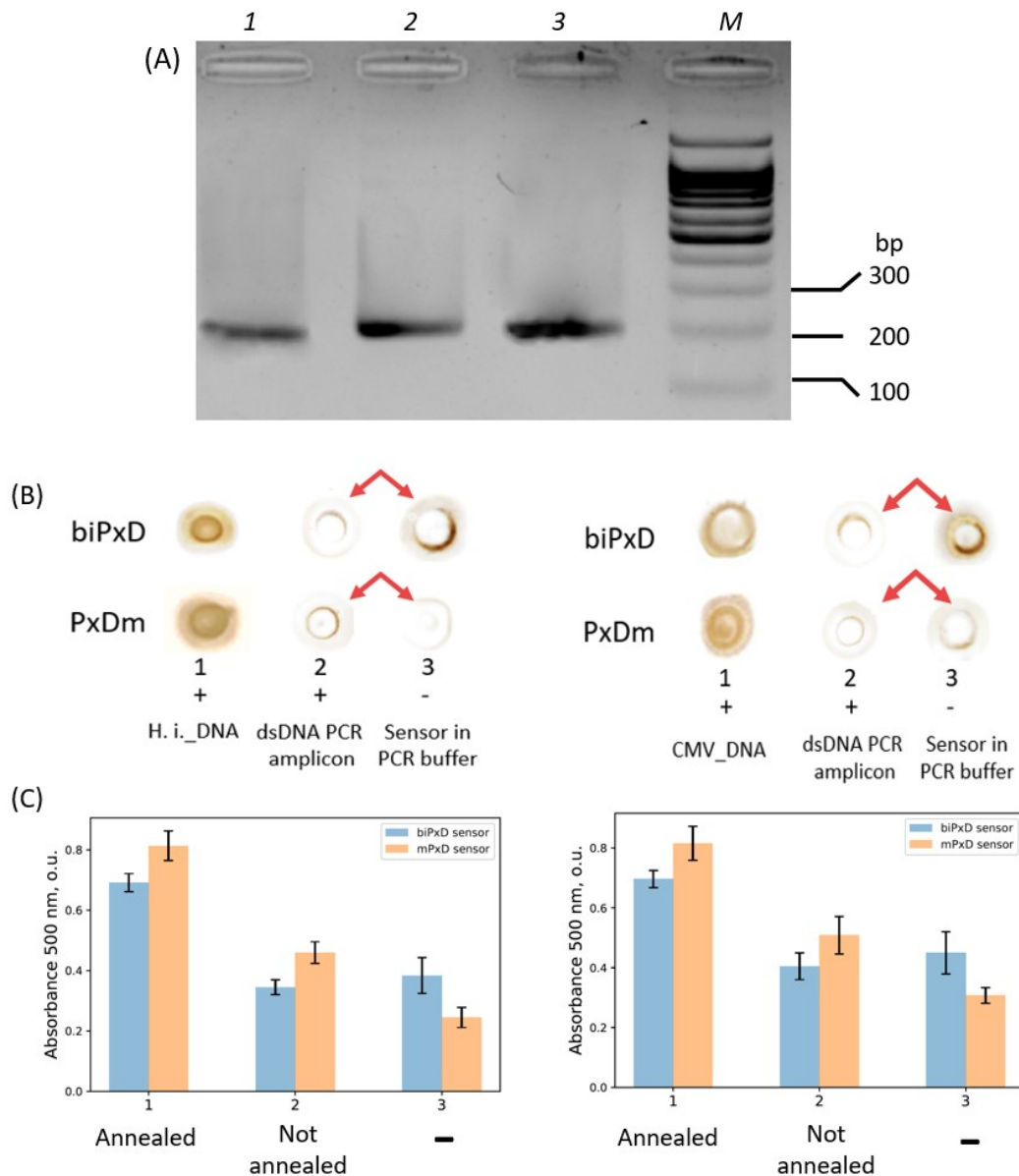


Fig. S7. Analysis of RT-PCR reaction mixtures by agarose and PxDM sensors. A) RT-PCR amplification of 1- *L.monocytogenes*, 2- *H.influenzae*, 3- Cytomegalovirus. B) Visual detection of *H.influenzae*, Cytomegalovirus RT-PCR amplicons by binary (biPxD) and multicomponent (PxDM) sensor in comparison with annealed at 95°C RT-PCR product (1 μ M) and negative control (PCR mixture with reagents and sensor without bacterial RNA). Visualization of the color change in the reaction mixtures containing RT-PCR amplicons obtained from 100 cells of *H.influenzae* and Cytomegalovirus (Vero cell line). C) Absorbance measurements of negative RT-PCR control (sensor and reagents in RT-PCR mixture without bacterial RNA), annealed/non-annealed RT-PCR products of *H.influenzae*, Cytomegalovirus.

8. Principles of PxDM sensor design, Fig. S8, S9 and S10

Further, we will rely on the RNA conformation predicted in the Unafold program. We selected a 20-40 nucleotide hairpin that is stable at ambient temperature to position the sensor. The multicomponent peroxidase-like DNA enzyme hybridization probe (PxDM) combines biPxDM and DNA nanoplatform technology. In this approach, the advantage of the two-analyte binding arms bound to a dsDNA platform is provided by PxDM. On one hand, the platform maintains that the two arms are separated to decrease their association. When the complex with the analyte is formed, contrariwise, it places the arms at the proper distance. PxDM's third arm binds the complex from the solution, allowing for highly selective analyte detection. Short analyte binding arms are used in this design, which lowers the probability of each arm folding into stable intramolecular structures or forming complexes with other arms or non-specific nucleic acids in the solution. When the two short DNA binding arms hybridize with abutting positions of the analyte, they form the G-4 structure. G-4 binds hemin and catalyzes the oxidation of the colorless substrate (e.g. diaminobenzidine) to a colored product in the presence of H_2O_2 . The brownish coloration indicates the target pathogen's presence in the analyzed biomaterial, which can be detected without additional equipment.

There are some following guiding principles that we established to ensure that PxDM achieves high performance:

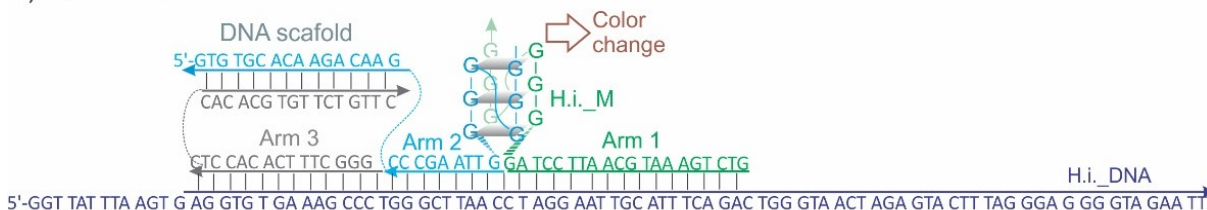
- 1) The long DNA platform (>20 bp) is more stable and enables the binding arms to be positioned appropriately to unwind the analyte. However, this platform is more expensive and requires a longer time for synthesis. The bulkiness may also have an impact on the efficacy of probe arms hybridization.
- 2) A short DNA platform (<20 bp) has the following benefits relative to a long one: it has been shown in an experiment that it can be sufficiently stable at 22°C and still much cheaper and less bulky. According to these facts, the short platform is more versatile and mobile in solutions. However, the 4 or 5 analyte-binding hands cannot be attached elegantly in this case.
- 3) Cross-hybridization of analyte-binding arms should be avoided. It makes no sense to make a short analyte binding arm in strand m if there is no need to detect a point mutation. T1 and T2 are supposed to form a stable hybrid. Here the law of turn can also be profitable: 10/21/31/42 base pairs per turn and 5/16/26/36- for 0.5, 1.5, 2.5, and 3.5 turns.
- 4) In order to create the most successful configuration, we avoided the stretch of more than 4 consequent complementarity base pairs for intramolecular interactions and more than 7 for interactions between 2 chains. It is preferable to have G-C pairs at the ends of the T1/T2 duplexes since it was established that the A-T pairs are not reliable at the ends of the duplex.⁹

Likewise, three designs of PxDM for detection *H. influenzae*, and Cytomegalovirus were developed (Fig. S8). Since *L. monocytogenes* and Cytomegalovirus turned out to be the most complicated for biPxDM detection due to the challenging arrangement of the analyte hairpins; designing PxDM probes needed extra ingenuity. As in the biPxDM design, the structure of the analyte binding arms was roughly retained. Several ttt or ccc bases have been used to link parts of the DNA platform to analyte-binding arms. The analyte-binding arms were linked to guanine-rich sequences through flexible oligo ethylene glycol linkers as in the biPxDM design.

It is worth mentioning that to assess the hairpin's stability, we used the criterion: the secondary structure's Gibbs energy does not exceed 4 kcal/mol. The criteria were defined experimentally, though not systematically.

The designs of PxDM sensors are shown in Fig. S6. The results of PxDM machine assembly in 2 % agarose gel electrophoresis in 1×TBE, 30 min, 80 V are shown in Fig. S9). The expected size of the machines in all cases is approximately 200 bp (Fig. S9).

A) *H.influenzae*



B) *Cytomegalovirus*

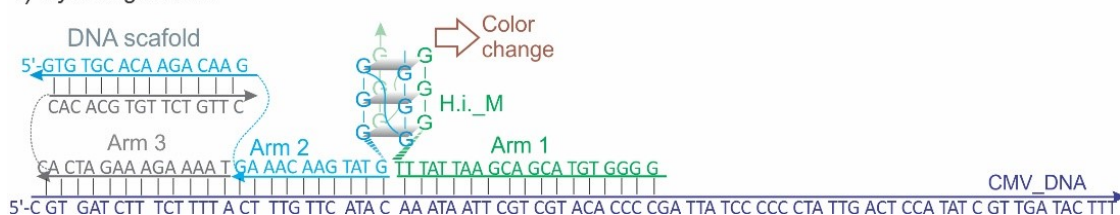


Fig. S8. Design of the PxDm probes targeting the gene fragments of *H.influenzae* and *Cytomegalovirus*. The probes in complex with their cognate analytes.

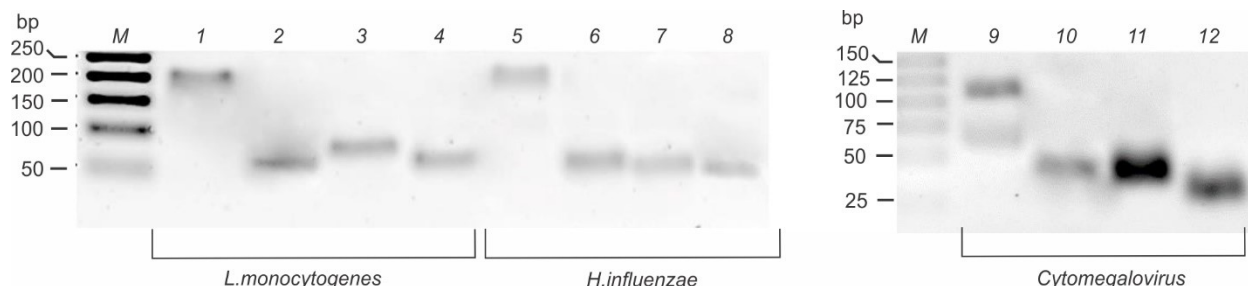


Fig. S9. Native gel analysis of the assembled PxDm machine for *L.monocytogenes*. M – ladder, 1 – PxDm machine for *L.monocytogenes*, 2 – L.m._T1_ PxDm, 3 – L.m._T2_ PxDm strand, 4 – L.m._F-7 strand. Native gel analysis of the assembled PxDm machine for *H.influenzae*. 5 – PxDm machine for *H.influenzae*, 6 – H.i._T1_ PxDm, 7 – H.i._T2_ PxDm, 8 – H.i._M_ PxDm strand. Native gel analysis of the assembled PxD machine for *Cytomegalovirus*. M – ladder, 1 – PxDm machine for *Cytomegalovirus*, 2 – CMV_T1_ PxDm strand, 3 – CMV_T2_ PxDm, 4 – CMV_M_ PxDm strand.

To demonstrate that PxDm is capable to invade to dsDNA without the annealing step, we prepared dsDNA strands, which correspond to the PCR amplicon by annealing L.m._DNA with same amount or with 2 times access amount of the complementary strand (L.m._DNA_antisense in Table S1) to ensure that there is no ssDNA analyte strand present in solution. The dsDNA analyte was then analyzed with the L.m._PxDm sensor. The data demonstrate equal signal ~3 times above the background for both complexes formed with the two stands annealed 1:1; and 1:2 ratio. This signal was expectedly lower than that in the presence of ssDNA analyte (blue bar in Fig 10C).

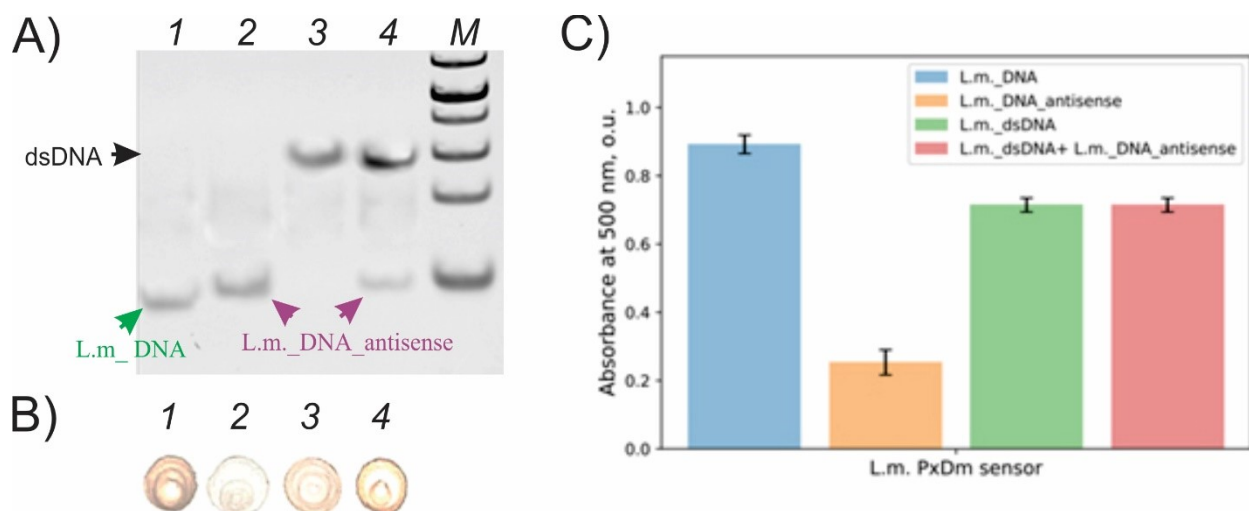


Fig. S10. Analysis of dsDNA by L.m. PxDM sensor. A) Analysis of DNA in 12% native PAGE analysis (2 h, 80V). Lane 1: The original L.m._DNA sequence; Lane 2: L.m._antisense, DNA Complementary sequence to L.m._DNA; lane 3: Solution of L.m._DNA + L.m._DNA_antisense, annealed at the ratio of 1:1 (equimolar concentration); Lane 4: solution with L.m._DNA + L.m._DNA_antisense, annealed and ratio of 1:2 respectively. B) Visual detection of the (i), (ii), (iii), (iv) analytes, respectively. C) Absorbance measurements(i), (ii), (iii), (iv) analytes, respectively. Note that L.m._DNA_antisense, was 6 nt longer to achieve separation in gel and clear differentiation from L.m._DNA

9. References

- 1 Rules for conducting of preanalytical stage. 2020. №53079. p. 4-2008.
<https://gosthelp.ru/gost/gost48362.html>
- 2 M. Drancourt, C. Bollet, A. Carlioz, R. Martelin, J.-P. Gayral, and D., *J. Clin. Microbiol.*, 2000, **38**, 3623-3630.
- 3 S. Mignard, J. P. Flandrois and J. Microbiol, *Methods*, 2016, **67**, 574-581.
- 4 D. Aggarwal, T. Kanitkar, M. Narouz et al., *Sci. Rep.*, 2020, **10**, 7965.
- 5 P. Bozidis, C. Williamson and A. Colberg-Poley A, *J. Virol.*, 2008, **82**, 715-2726.
- 6 M. Deckers, J. Hofmann, K.A. Kreuzer *J. Virol.*, 2009, 210.
- 7 J. Compton, *Nature*, 1991, **350**, 91-2.
- 8 N.R. Markham and M. Zuker, *Methods Mol Biol.*, 2008, **8**, 453, 3-31.
- 9 E. A. Kovtunov, L. A. Shkodenko, E. A. Goncharova, D. D. Nedorezova, S. V. Sidorenko, E. I. Koshel and D.M. Kolpashchikov, *ChemistrySelect*, 2020, **5**, 14572 –14577.
- 10 A. Idili, F. Ricci, A. Vallée-Bélisle, *Nucl. Acids Res.*, 2017, **45**, 7571–7580. R. P. Connelly, C. Verduzco,
- 11 D. M. Kolpashchikov, *J. Am. Chem. Soc.*, 2008, **130**, 2934–2935
- S.T. Farnell and Y. V. Gerasimova, *ACS Chem. Biol.*, 2019, **14**, 2701–2712.